SUPPLEMENTARY INFORMATION

Convection Enhanced Phase Change Composite Fibers for Advanced Thermal Management

Yu Du[1†], Siyuan Ding[2,3†], Yueni Zhong[1], Fangzheng Zhen[1], Ming Yong[4,5], Yinghui Wu[1], Zihan Chen[1], Weiren Fan[1], Qijun Zheng[1,5], Ean Hin Ooi[6], Baofu Ding[7], Sheng Yan[8], Jianli Wang[9], Ruiping Zou[*1], Ling Qiu[*3], Aibing Yu[10,11], Minsu Liu[*1,5,12]

[1]ARC Research Hub for Smart Process Design and Control, Department of Chemical Engineering, Monash University, VIC 3800, Australia.

[2]School of Energy and Environment, Southeast University, Nanjing 210096, China

[3]Tsinghua Shenzhen International Graduate School (TSIGS), Tsinghua University, Shenzhen 518055, China

[4]UQ Dow Centre for Sustainable Engineering Innovation, School of Chemical Engineering, The University of Queensland, St Lucia, QLD 4072, Australia.

[5]Monash Suzhou Research Institute, Monash University, Suzhou 215000, China

[6]Department of Mechanical Engineering, School of Engineering, Monash University Malaysia, Jalan Lagoon Selatan, Bandar Sunway, 47500, Subang Jaya, Selangor, Malaysia

[7]Institute of Technology for Carbon Neutrality, Shenzhen Institute of Advanced Technology, Chinese Academy of Sciences, Shenzhen 518055, China

[8]Institute for Advanced Study, Shenzhen University, Shenzhen 518000, China

[9]Jiangsu Key Laboratory for Design and Manufacturing of Precision Medicine Equipment, Department of Mechanical Engineering, Southeast University, Nanjing 210096, China

[10]Centre for Simulation and Modelling of Particulate Systems, Southeast University, Suzhou 215000, China

[11]Research Center for Smart Process Engineering, Great Bay University, Dongguan 523000, China

[12]Department of Materials Science and Engineering, Monash University, VIC 3800, Australia.

*Corresponding Authors: Ruiping Zou (ruiping.zou@moansh.edu), Ling Qiu (ling.qiu@sz.tsinghua.edu.cn), and Minsu Liu (minsu.liu1@monash.edu)

†These authors contributed equally to this work.

Keywords: Phase Change Martials; Thermal Convection; Core-Shell Structure; Fiber; Thermal Management

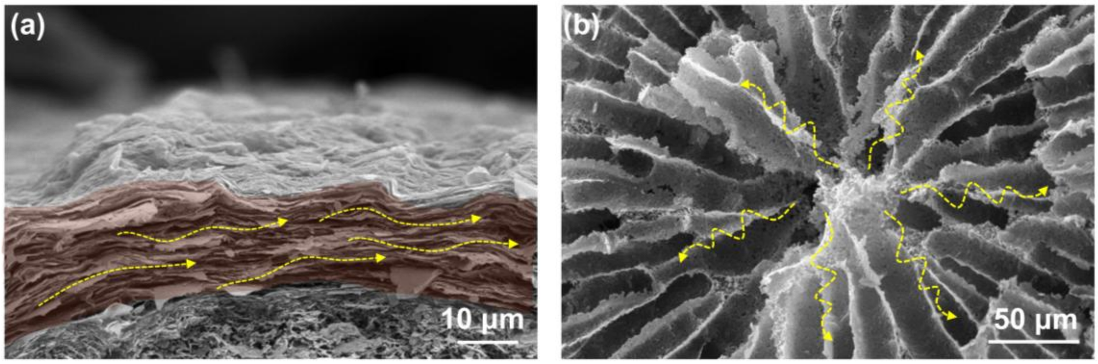

Fig. S1: Enlarged SEM image of (**a**) dense shell and (**b**) porous core with yellow arrow shows the heat transfer path.

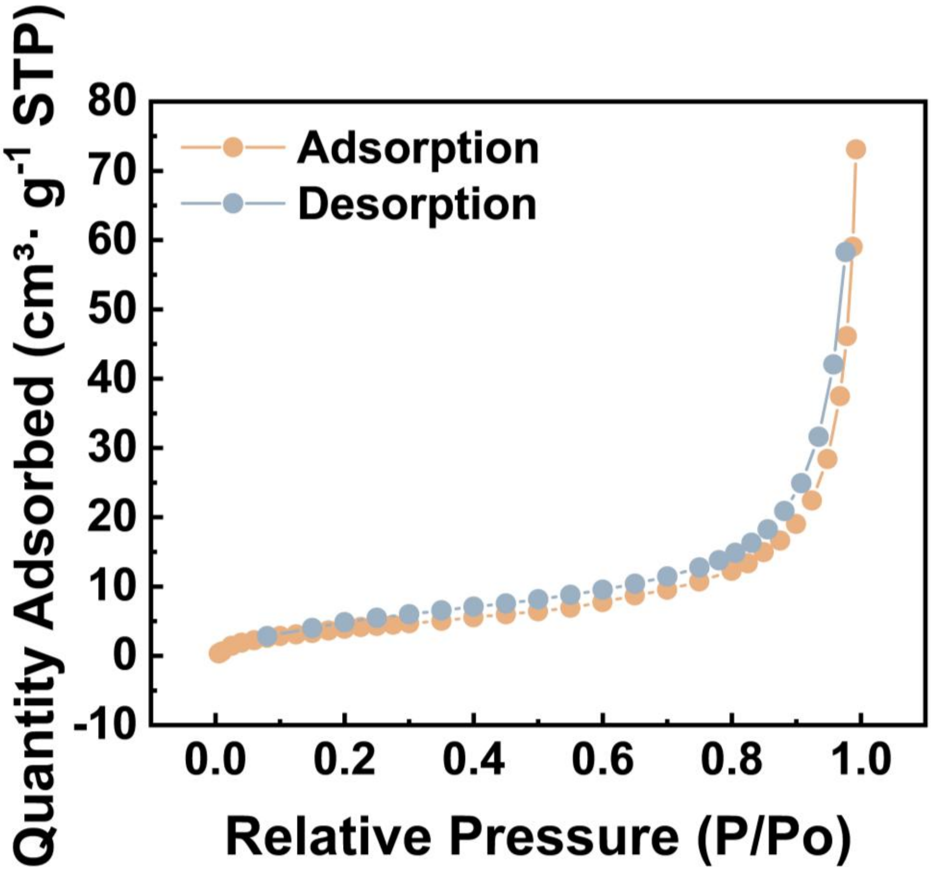

Fig. S2: BET adsorption–desorption curves of porous medium.

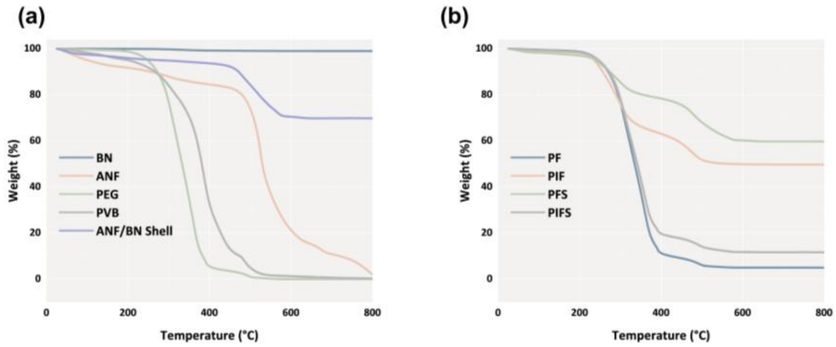

Fig. S3: TGA result of each samples.

Calculation result:

ANF/BN shell consists of 70 wt% ANF and 30 wt% BNNS;

PF consists of 50wt% PVB and 50 wt% of BNNS;

PFS consists of 50 wt% PM core and 50 wt% ANF/BN shell;

PIF consists of 90 wt% PEG and 10 wt% PM;

PIFS consists of 5 wt% PM core, 5 wt% ANF/BN shell and 90wt% PEG.

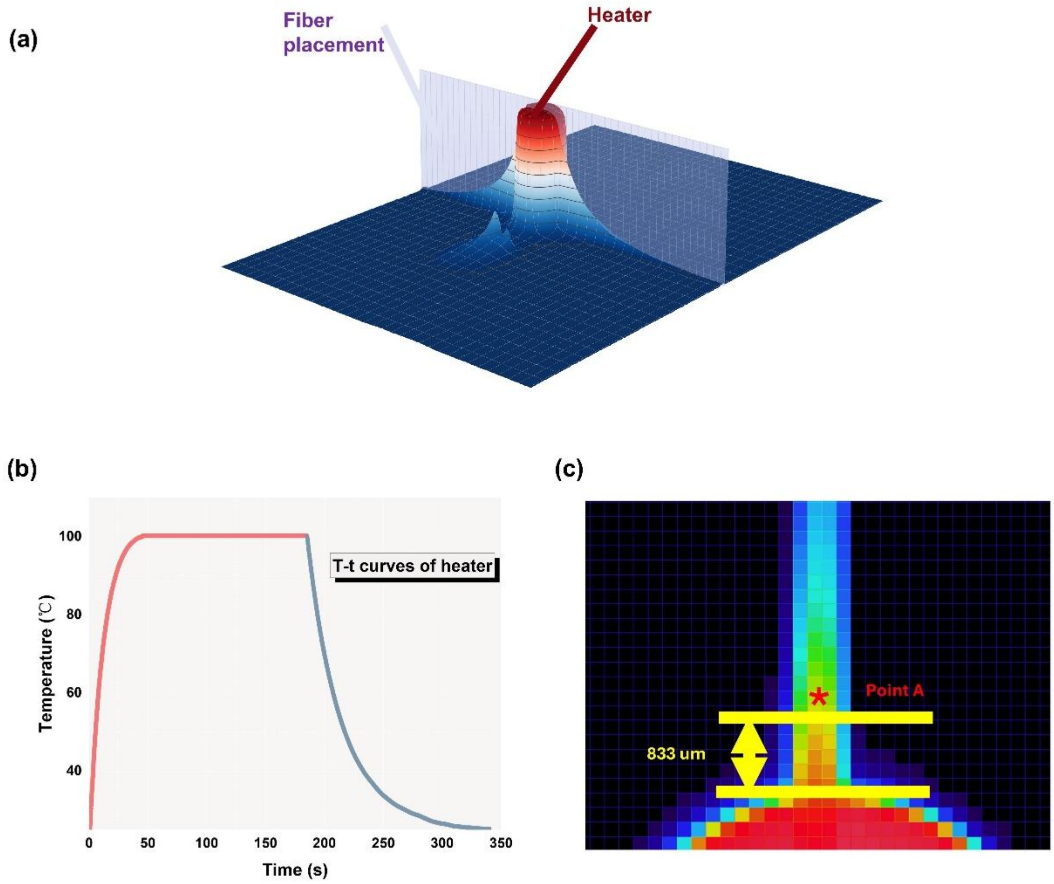

Fig. S4: Setup of the Thermal test for fibers. **(a)** The relative position of the fibre and the heater;(**b)** The temperature profile of the heater;**(c)** The selection of equidistant point.

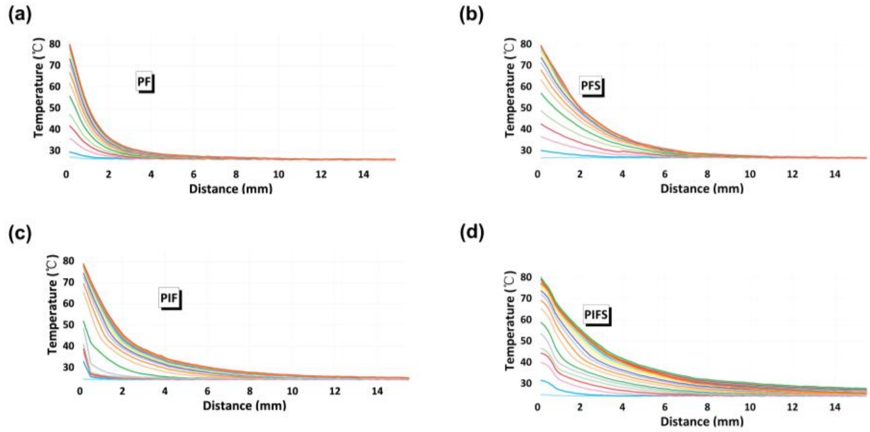

Fig. S5: Comparison of the temperature distribution curves along the fibers along the time

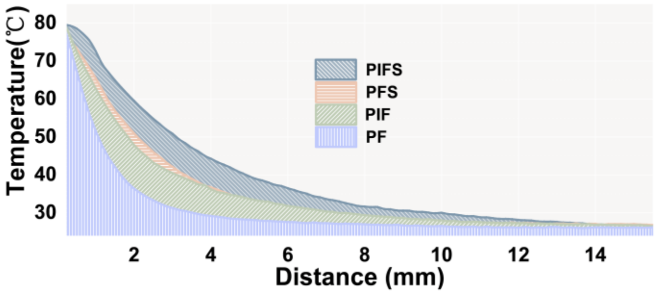

Fig. S6: A steady-state temperature distribution curve comparison along the fibers

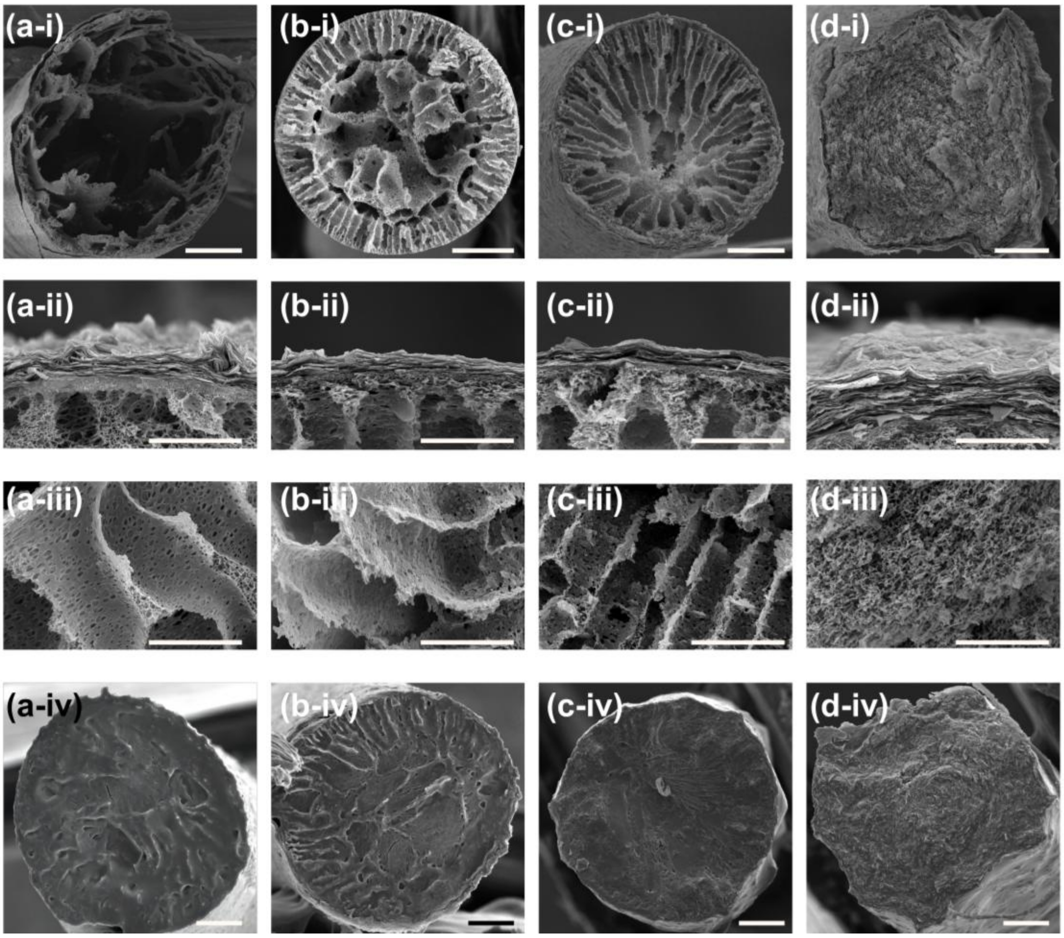

Fig. S7: SEM images of **(a)** PFS-1; **(b)** PFS-3; **(c)** PFS-5; **(d)** PFS-7. Amon them, **(i)** the cross section, scale bar 100 μm and **(ii)** outer shell, scale bar 30 μm; **(iii)** enlarged image on porous structure, scale bar 30 μm; **(iv)**after filled with PCM, scale bar 100 μm.

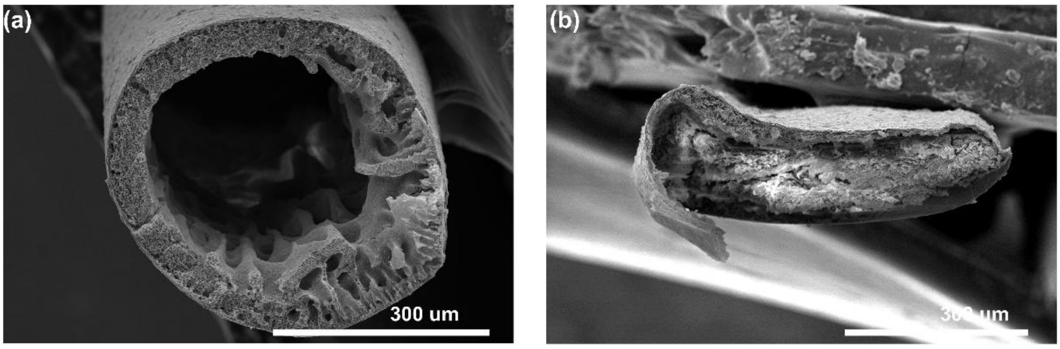

Fig. S8: SEM cross section of **(a)** PFS-0 and **(b)** PFS-9

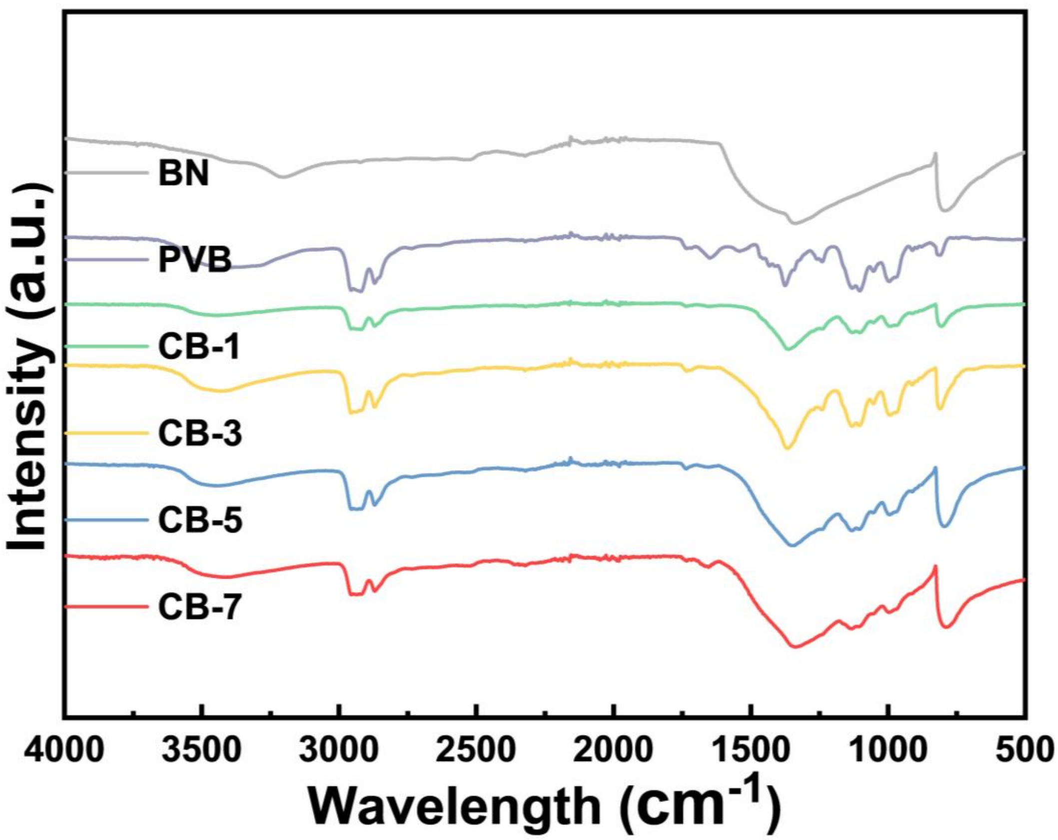

Fig. S9: FTIR spectra of samples. Noted CB-X was assigned as a porous fiber obtained by uniaxial spinning of PVB/BNNS according to the concentration of BNNS in the core from 10% to 70%.

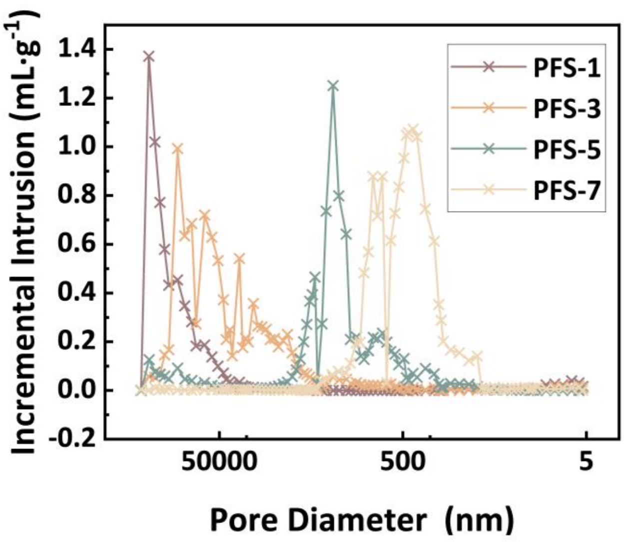

Fig. S10: Pore size distributions of PFSs.

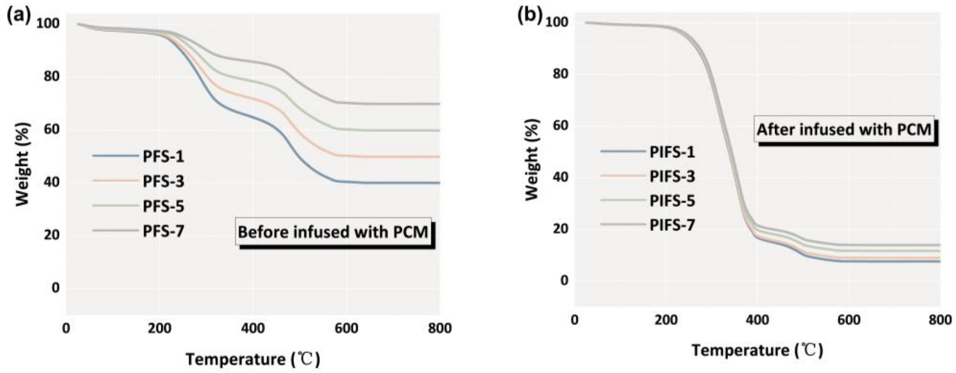

Fig. S11: TGA result of each samples **(a)** before and **(b)** after infused with PCM.

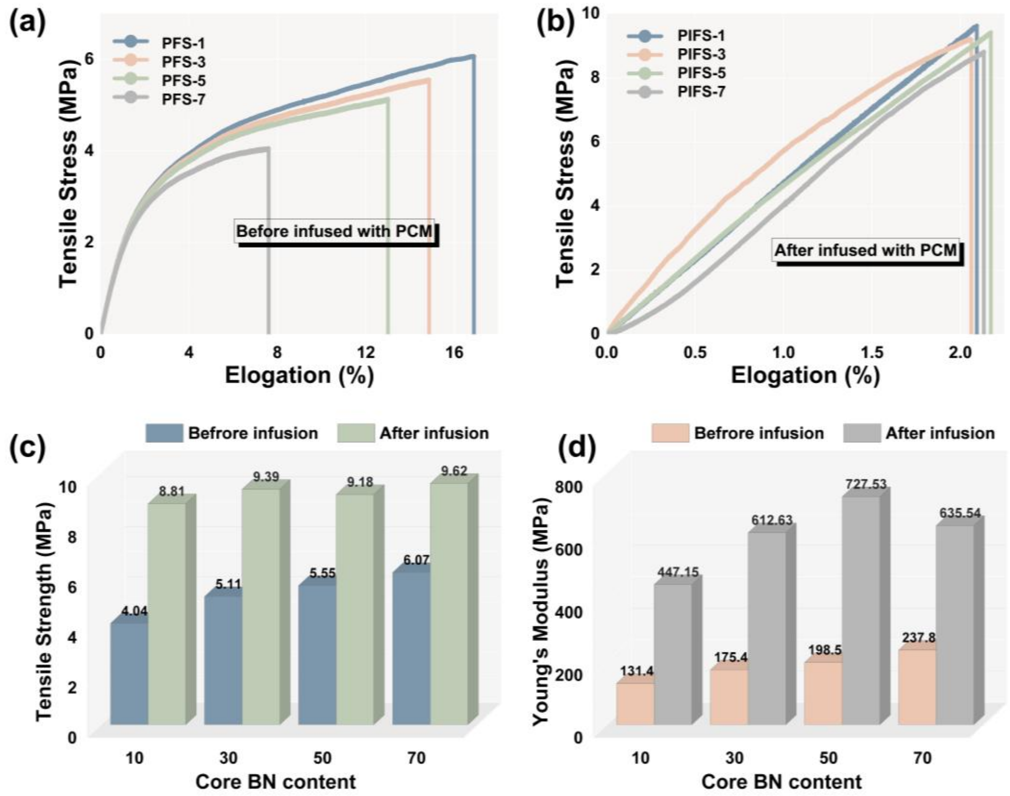

Fig. S12: Stress-strain curves of samples **(a)** before and **(b)** after infused with PCM; **(c)** Tensile strength and **(d)** Young's of samples before and after infused with PCM.

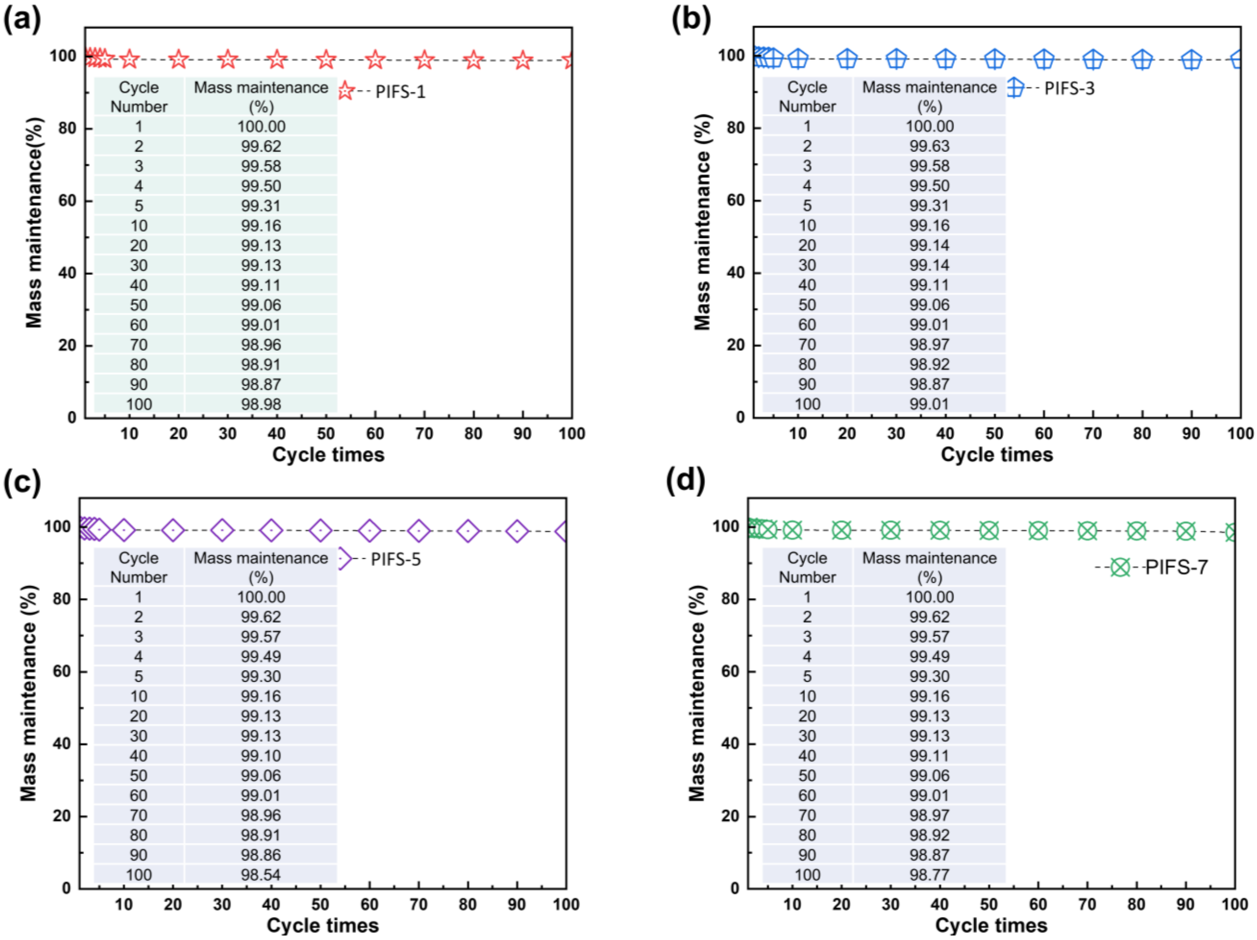

Fig. S13: Mass maintenance of each sample after thermal cycles. **(a)** PIFS-1; **(b)** PIFS-3; **(c)** PIFS-5; **(d)** PIFS-7.

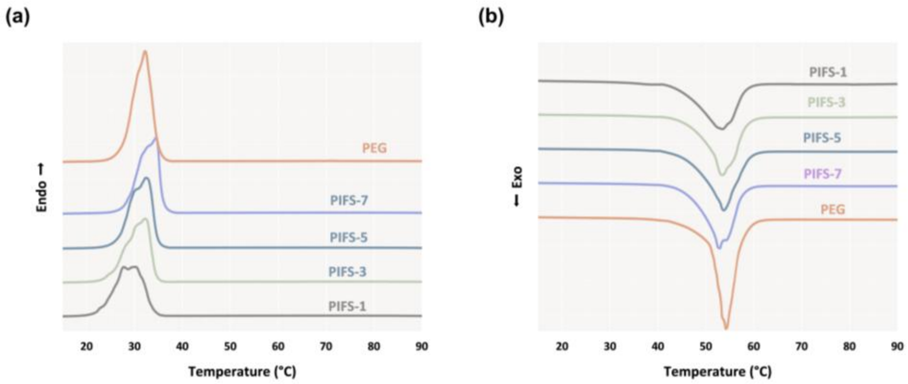

Fig. S14 : DSC curves of each sample **(a)** Endo and **(b)** Exo.

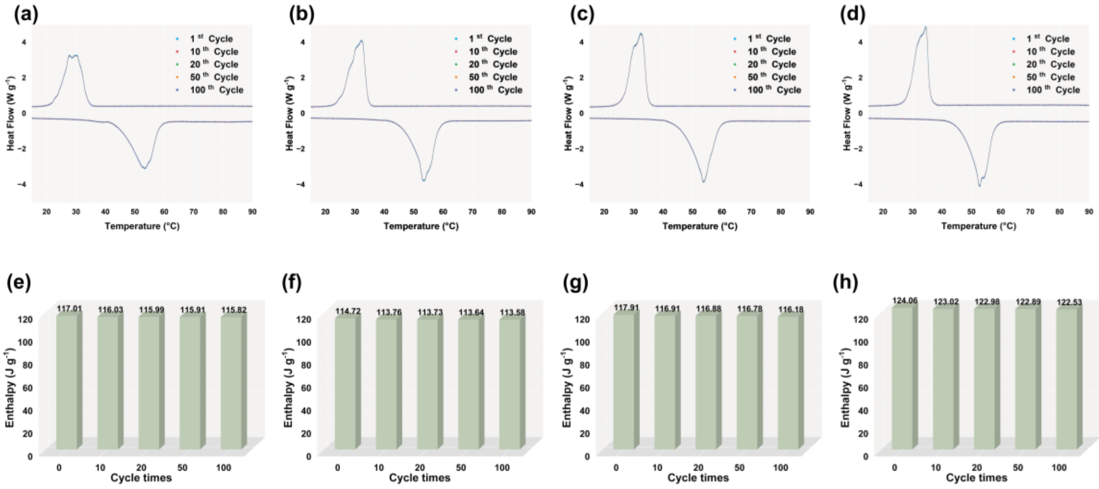

Fig. S15: DSC curves **(a)** PIFS-1; **(b)** PIFS-3; **(c)** PIFS-5; **(d)** PIFS-7. and enthalpy **(e)** PIFS-1; **(f)** PIFS-3; **(g)** PIFS-5; **(h)** PIFS-7. of each sample after different thermal cycles.

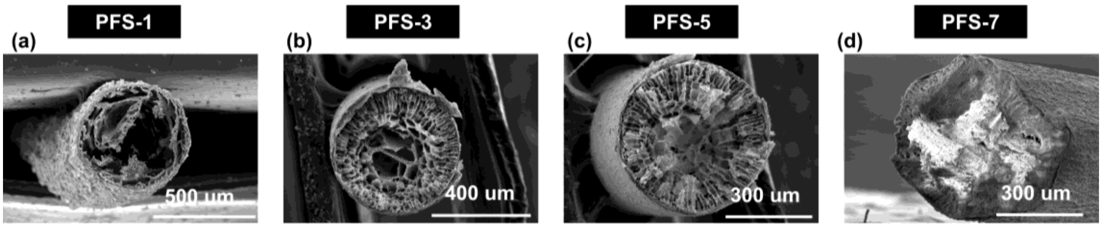

Fig. S16 : Core@shell fiber after 100 times thermal cycle PEG removed by water. **(a)** PFS-1; **(b)** PIFS-3; **(c)** PIFS-5; **(d)** PIFS-7.

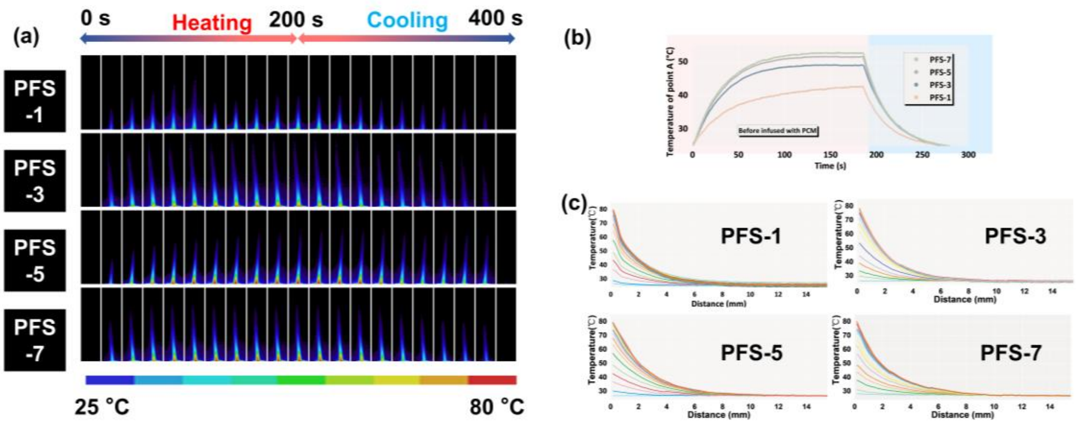

Fig. S17: **(a)**Thermal images and **(b)**Temperature-time and **(c)**Temperature-distance curves of fibers before infused with PCM.

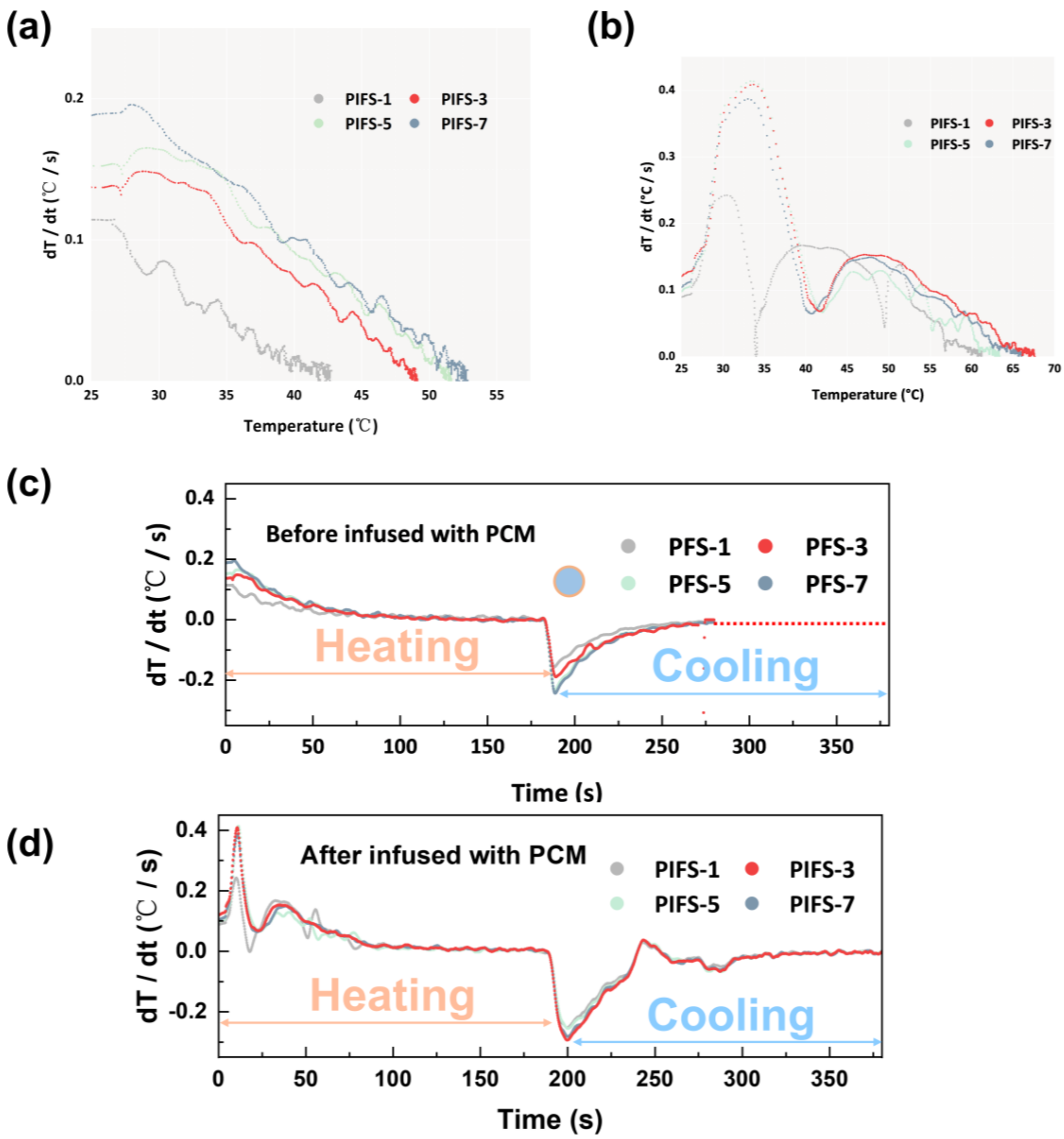

Fig. S18: Temperature differential curves dT/dt vs. T of fibers **(a)** before and **(b)** after infused with PCM; Temperature differential curves dT/dt vs. t of fibers **(c)** before and **(d)** after infused with PCM.

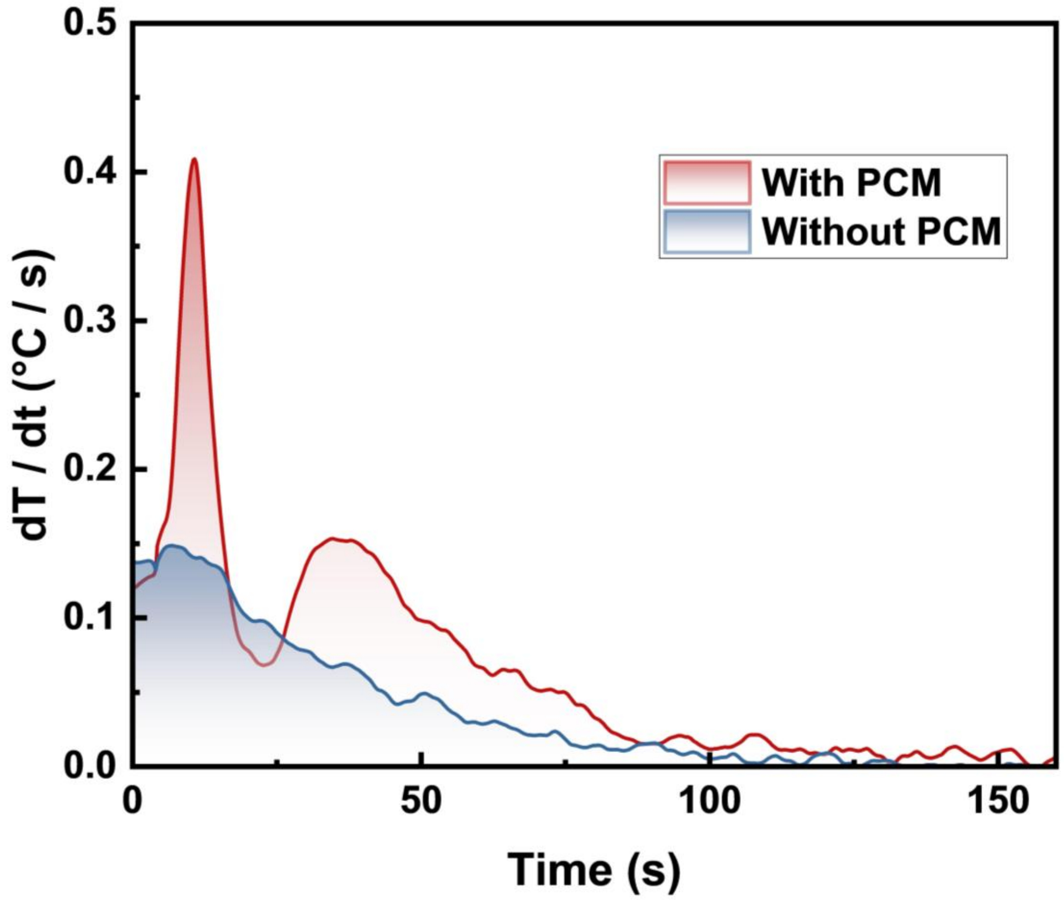

Fig. S19: Temperature differential curves dT/dt vs. time of PIFS-3 before and after infused with PCM

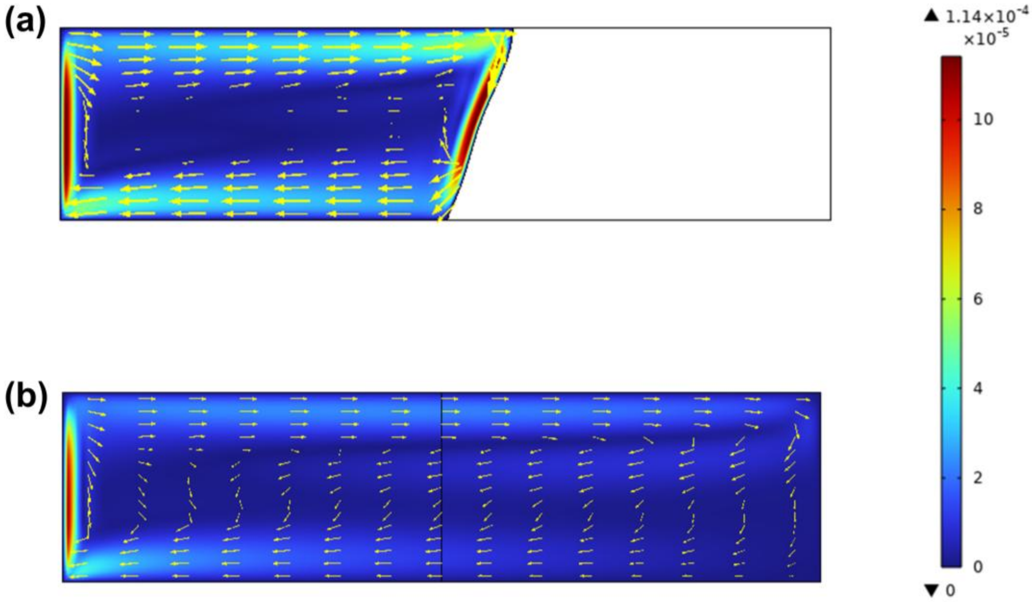

Fig. S20: Velocity clouds and vectors (yellow arrows) of the fluid in the **(a)** melting **(b)** liquid stages.

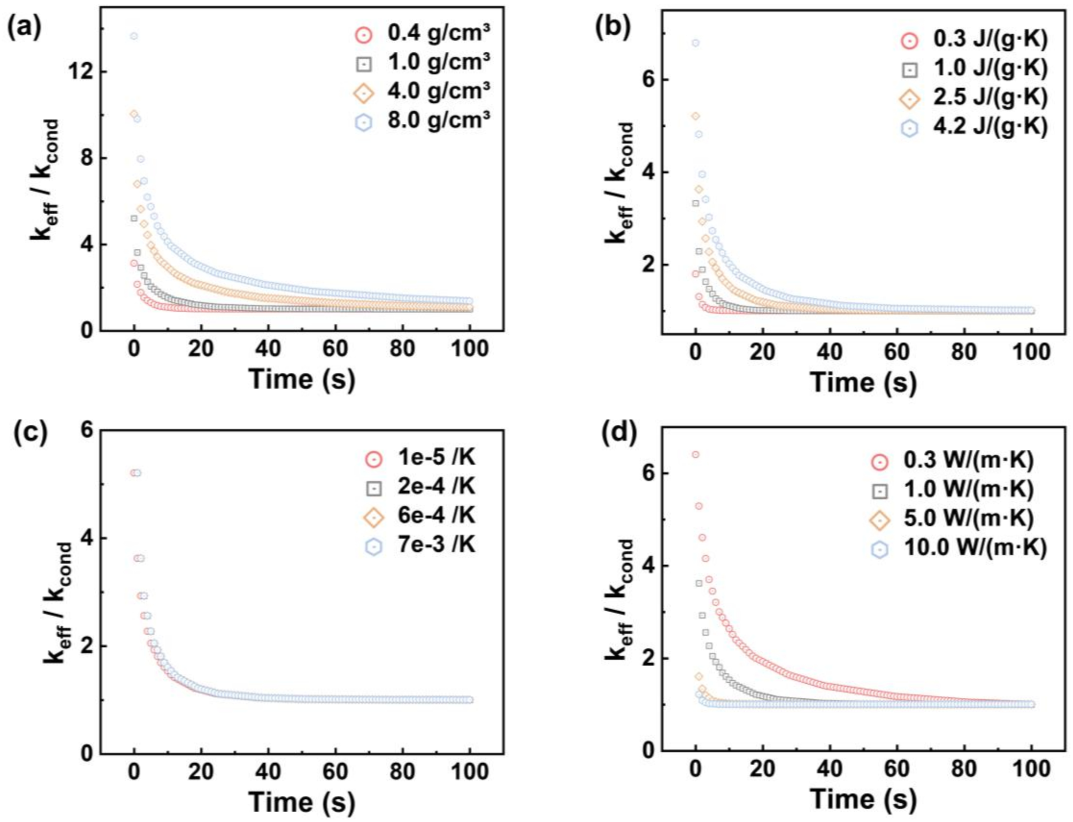

Fig. S21: Nusselt coefficients for different fluid characteristics: **(a)** density; **(b)** heat capacity; **(c)** thermal expansion coefficient; **(d)** thermal conductivity.

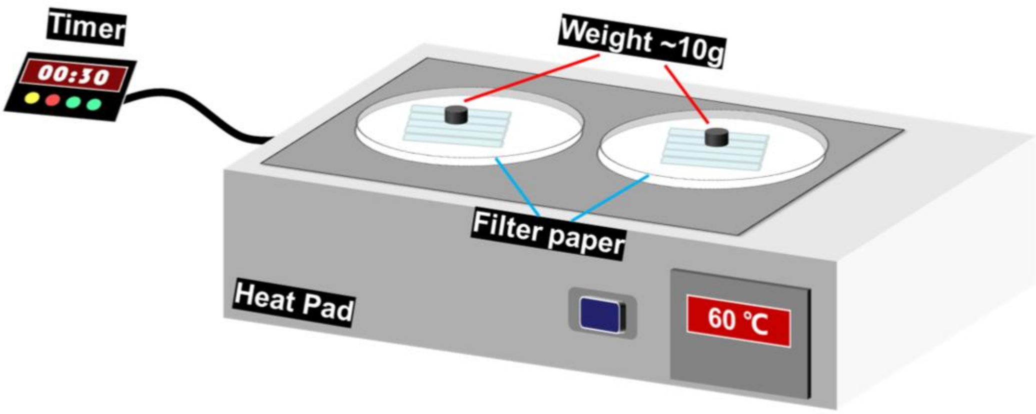

Fig. S22 : Setup of the cyclic thermal test.

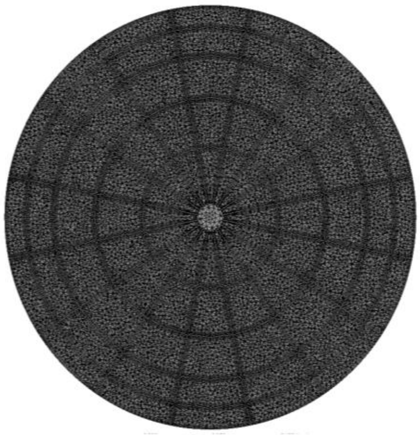 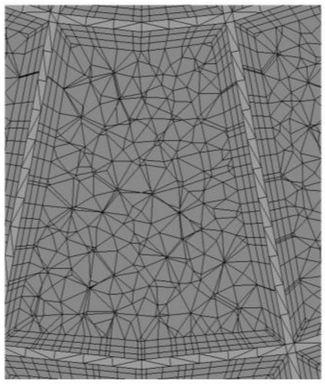

Preset sizes	6.25 μm
Quality	0.88 skewness
Boundary layers	3 layers
Thick mesh	688073 grids
Thin mesh	1389607 grids

Fig. S23 : Mesh configuration for the simulation

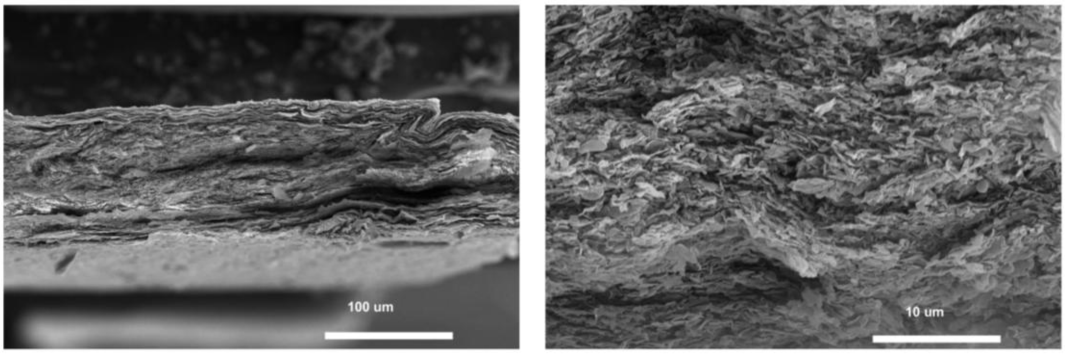

Fig. S24 : SEM of the porous core after hot-pressing.

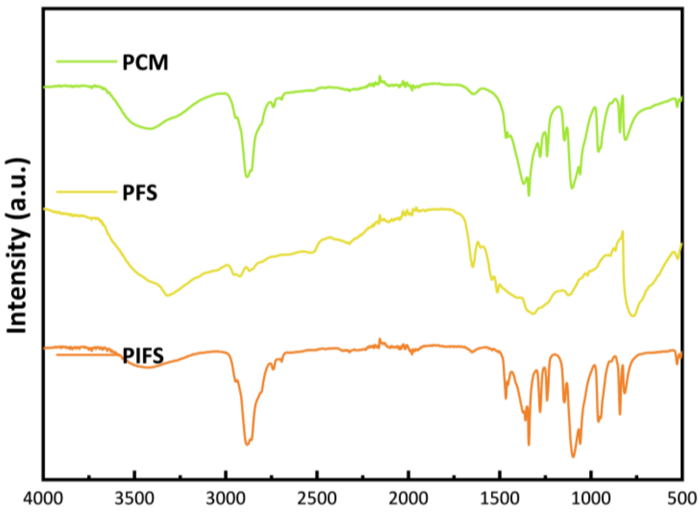

Fig. S25 : FTIR spectra of the fibers before and after the filled with PCM.

Tab. S1: Thermal conductivity of fibers before infused with PCM

Sample	**PF**	**PFS-1**	**PFS-3**	**PFS-5**	**PFS-7**
Density ($\times 10^3$ g cm^{-3})	0.07	0.09	0.10	0.12	0.15
Specific heat capacity ($\times 10^3$ J kg^{-1} K^{-1})	1.03	1.17	1.16	1.15	1.15
Suspended length L_1 (um)	3225	3452	3321	2902	3290
Diameter D_1 (um)	358	362	342	361	351
$\alpha_{\text{real+radiation 1}}$ ($\times 10^{-6}$ m^2 s^{-1})	1.01	13.99	12.63	13.08	14.86
Suspended length L_2 (um)	4386	4216	4258	4598	4038
Diameter D_2 (um)	371	358	363	352	360
$\alpha_{\text{real+radiation 2}}$ ($\times 10^{-6}$ m^2 s^{-1})	1.69	17.04	15.02	20.66	17.87
α_{real} ($\times 10^{-6}$ m^2 s^{-1})	0.15	7.99	8.27	8.27	8.42
Thermal Conductivity (W m^{-1} K^{-1})	0.01	0.85	0.98	1.16	1.49

Tab. S2: Thermal conductivity of fibers after infused with PCM

Sample	**PIF**	**PIFS-1**	**PIFS-3**	**PIFS-5**	**PIFS-7**
Density ($\times 10^3$ g cm^{-3})	1.01	1.03	1.04	1.04	1.04
Specific heat capacity ($\times 10^3$ J kg^{-1} K^{-1})	2.21	2.23	2.23	2.23	2.23
Suspended length L_1 (um)	3046	3650	3662	3261	3477
Diameter D_1 (um)	389	386	401	394	413
$\alpha_{\text{real+radiation 1}}$ ($\times 10^{-6}$ m^2 s^{-1})	1.87	24.40	31.63	20.10	29.36
Suspended length L_2 (um)	4724	4023	4235	4753	4538
Diameter D_2 (um)	376	399	420	406	424
$\alpha_{\text{real+radiation 2}}$ ($\times 10^{-6}$ m^2 s^{-1})	4.35	28.47	40.26	40.87	48.27
α_{real} ($\times 10^{-6}$ m^2 s^{-1})	0.21	0.38	0.45	0.53	0.67
Thermal Conductivity (W m^{-1} K^{-1})	0.46	0.89	1.05	1.22	1.55